




Article

Chemical Fingerprinting and Biological Evaluation of the Endemic Chilean Fruit *Greigia sphacelata* (Ruiz and Pav.) Regel (Bromeliaceae) by UHPLC-PDA-Orbitrap-Mass Spectrometry

Ruth E. Barrientos ^{1,†} , Shakeel Ahmed ^{1,†}, Carmen Cortés ¹, Carlos Fernández-Galleguillos ¹, Javier Romero-Parra ², Mario J. Simirgiotis ^{1,*}  and Javier Echeverría ^{3,*} 

¹ Instituto de Farmacia, Facultad de Ciencias, Universidad Austral de Chile, Valdivia 5090000, Chile; ruth.barrientos@alumnos.uach.cl (R.E.B.); shakeel.ahmed@uach.cl (S.A.); carmenc1012@gmail.com (C.C.); carlos.fernandez@uach.cl (C.F.-G.)

² Departamento de Química Orgánica y Físicoquímica, Facultad de Ciencias Químicas y Farmacéuticas, Universidad de Chile, Olivos 1007, Casilla 233, Santiago 8380544, Chile; javier.romero@ciq.uchile.cl

³ Departamento de Ciencias del Ambiente, Facultad de Química y Biología, Universidad de Santiago de Chile, Casilla 40, Correo 33, Santiago 9170002, Chile

* Correspondence: mario.simirgiotis@gmail.com or mario.simirgiotis@uach.cl (M.J.S.); javier.echeverriam@usach.cl (J.E.); Tel.: +56-63-63233257 (M.J.S.); +56-2-27181154 (J.E.)

† These authors contributed equally to this study.

Received: 20 July 2020; Accepted: 14 August 2020; Published: 17 August 2020



Abstract: *Greigia sphacelata* (Ruiz and Pav.) Regel (Bromeliaceae) is a Chilean endemic plant popularly known as “quiscal” and produces an edible fruit consumed by the local Mapuche communities named as “chupón”. In this study, several metabolites including phenolic acids, organic acids, sugar derivatives, catechins, proanthocyanidins, fatty acids, iridoids, coumarins, benzophenone, flavonoids, and terpenes were identified in *G. sphacelata* fruits using ultrahigh performance liquid chromatography-photodiode array detection coupled with a Orbitrap mass spectrometry (UHPLC-PDA-Orbitrap-MS) analysis for the first time. The fruits showed moderate antioxidant capacities (i.e., 487.11 ± 26.22 $\mu\text{mol TE/g}$ dry weight) in the stable radical DPPH assay, 169.08 ± 9.81 TE/g dry weight in the ferric reducing power assay, 190.32 ± 6.23 TE/g dry weight in the ABTS assay, and $76.46 \pm 3.18\%$ inhibition in the superoxide anion scavenging assay. The cholinesterase inhibitory potential was evaluated against acetylcholinesterase (AChE) and butyrylcholinesterase (BChE). From the findings, promising results were observed for pulp and seeds. Our findings suggest that *G. sphacelata* fruits are a rich source of diverse secondary metabolites with antioxidant capacities. In addition, the inhibitory effects against AChE and BChE suggest that natural products or food supplements derived from *G. sphacelata* fruits are of interest for their neuroprotective potential.

Keywords: *Greigia sphacelata*; endemic fruits; UHPLC-PDA-Orbitrap-MS; metabolomic analysis; antioxidant; cholinesterase inhibition

1. Introduction

Plant-based foods, especially fruits, have a great impact on human health [1,2]. Indeed, there is a growing body of scientific literature describing curative effects of fruits against a broad spectrum of diseases including diabetes, obesity, neurodegenerative, gastric and cardiovascular disorders, and certain types of cancers [3–6]. Different types of secondary metabolites have been reported in fruits [4,7–9]. These compounds are in part responsible for their biological properties.

The genus *Greigia* (Bromeliaceae) comprise approximately 36 species in Central and South America and form an extraordinary disjunct distribution in humid habitats. Among Chilean *Greigia*, four endemic species have been described: *G. pearcei* (Mez), *G. landbeckiia* (Lechl. ex Phil.) F.Phil., *G. berteroi* (Skotts.) and *G. sphacelata* (Ruiz and Pav.) Regel. *Greigia sphacelata* (Ruiz and Pav.) Regel (Bromeliaceae) (local name: Chupon and quiscal) is an endemic plant (Figure 1a,b) widely distributed in temperate zones of Central and Southern Chile [10].



Figure 1. *Greigia sphacelata* (Ruiz and Pav.) Regel (Bromeliaceae). (a) Fruits, (b) plant.

The edible fruits of *G. sphacelata* are juicy, sweet, and with a similar flavor to apple and pineapple, and are eaten raw, or prepared as an infusion or as a fermented beverage. Few reports have investigated the chemical properties of *G. sphacelata*. From the aerial parts of *G. sphacelata* flavanones (5,7,3'-trihydroxy-6,4',5'-trimethoxyflavanone, and 5,3'-dihydroxy-6,7,4',5'-tetramethoxyflavanone), glycerol derivatives (1-*O*-*trans*-*p*-coumaroylglycerol, 1,3-*O*-di-*trans*-*p*-coumaroylglycerol, 1-(ω -feruloyl-docosanoyl) glycerol, and 1-(ω -feruloyl-tetracosanoyl) glycerol), and *trans*-ferulic acid, arborinone, 22-hydroxydocosanoic acid ester, isoarborinol and arborinol have been isolated and characterized [11]. To our knowledge, there are no reports on the chemical characterization or antioxidant and enzyme inhibitory properties of the natural products obtained from *G. sphacelata* fruits.

HPLC or UHPLC coupled to mass spectrometry is a key technique for plant chemotaxonomy or comparative metabolic profiling. Q-Exactive type focus equipment uses a very rapid high-performance mass spectrometer for the detection of small organic molecules [12–14]. This is a dual high resolution

with accurate mass (HRAM) spectrometer with an orbital trap (Orbitrap), a quadrupole (Q), and a high-performance collision cell (HCD), capable of producing high-resolution parent ions and diagnostic MS daughter fragments. The hyphenated ultrahigh performance liquid chromatography-photodiode array detection coupled with a Orbitrap mass spectrometry (UHPLC-PDA-Orbitrap-MS) approach is a key tool for the identification of secondary metabolites in plants and edible fruits [15–17].

In this work, we report the antioxidant activity, cholinesterase inhibitory potential plus the UHPLC-PDA-Orbitrap-MS fingerprinting from the endemic *G. sphacelata* fruits for the first time.

2. Results and Discussion

2.1. Metabolomic Analyses

In this study, the fingerprint was generated using UHPLC-PDA-Orbitrap-MS (Figure 2) allowing the determination of several types of metabolites in the fruits of the Mapuche specie *G. sphacelata* (Table 1). The metabolites identified include: Eleven phenolic acids (peaks 1, 6, 8, 13, 14, 16, 21, 42, 47, 48, and 54); six organic acids (peaks 2–5, 7, and 10, including a vitamin peak 7); eleven sugar derivatives (peaks 12, 15, 19, 22–24, 26, 31, 39, 40, and 59); five catechins and/or proanthocyanidins (peaks 34, 37, 41, 44, and 49); thirteen fatty acids, (peaks 33, 50, 52, 55, 56, 58, 62–67, and 69); four iridoids (peaks 11, 17, 18, and 68); three coumarins (peaks 25, 27, and 30); one benzophenone (peak 57); ten flavonoids (peaks 20, 28, 29, 32, 35, 36, 38, and 43–46); five terpenes, (peaks 9, 51, 53, 60, and 61).

Examples of full MS spectra and structures of the compounds identified are displayed in Figure S1. The detailed identification is explained below:

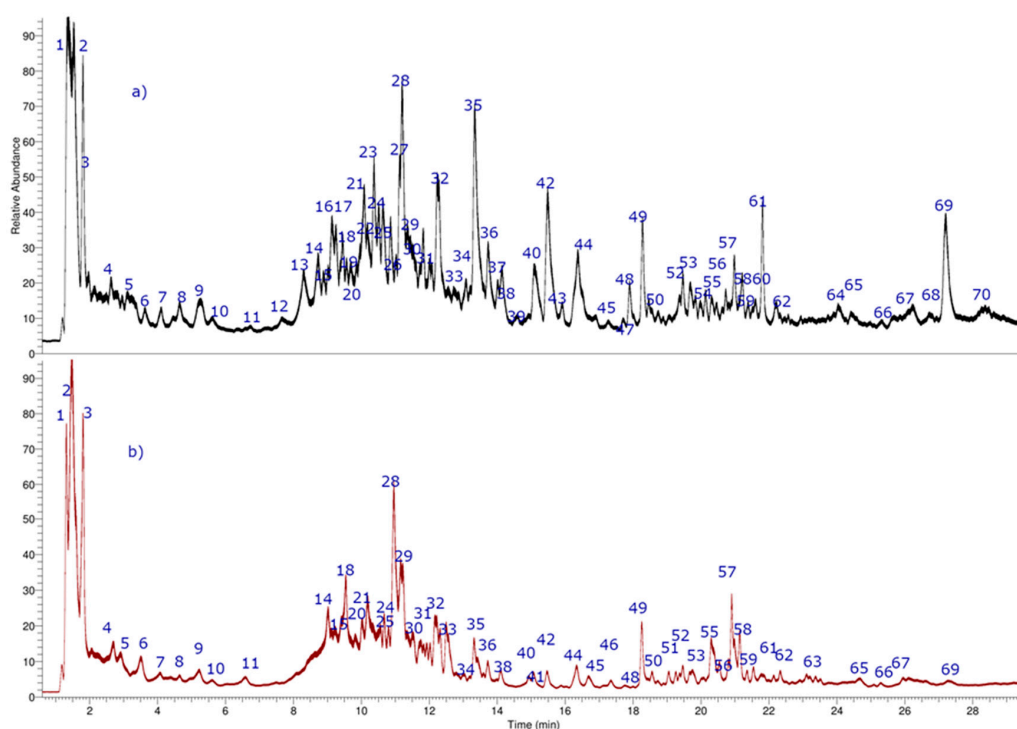


Figure 2. UHPLC chromatograms of *G. sphacelata* (a) pulp, and (b) seeds.

Table 1. Full metabolome identification in *Greigia sphacelata* by UHPLC-PDA-Orbitrap-MS.

Peak	Tentative Identification	[M – H] [–] Ions	Retention Time (min)	UV Max (nm)	Theoretical Mass (m/z)	Measured Mass (m/z)	Accuracy (ppm)	Metabolite Type	MS ² Ions (ppm)	Fruit Part
1	Syringaldehyde syringate	C ₁₈ H ₁₇ O ₉ [–]	1.36	315	377.08578	377.08671	–2.44	Pa	215.03258	P; S
2	Quinic acid	C ₇ H ₁₁ O ₆ [–]	1.45		191.05501	191.05621	3.16	Oa	135.02919	P; S
3	Citric acid	C ₆ H ₇ O ₇ [–]	1.52	187	191.01863	191.01915	3.12	Oa	162.89121, 111.00782	P; S
4	Dehydroascorbic acid	C ₆ H ₅ O ₆ [–]	2.20	176	173.00806	173.00879	4.18	Oa		P; S
5	Isocitric acid	C ₆ H ₇ O ₇ [–]	2.74		191.01863	191.01923	3.76	Oa	162.89110, 111.00810	P; S
6	Diffutidin	C ₁₇ H ₁₈ O ₅ [–]	3.45		301.10705	301.10614	–3.02	Pa	153.01875	P; S
7	Homocitric acid	C ₁₀ H ₁₇ O ₄ [–]	4.05		205.03542	205.03491	–2.43	Oa		P; S
8	Vanilloyl-glucoside	C ₁₄ H ₁₇ O ₉ [–]	4.34	287	329.08810	329.08671	4.24	Pa	151.03874, 123.02314	P; S
9	Euonyminol	C ₁₅ H ₂₅ O ₁₀ [–]	5.26		365.14422	365.14560	3.76	Te		P; S
10	Pantothenic acid	C ₉ H ₁₆ NO ₅ [–]	5.255		218.10230	218.10313	3.82	Oa	125.85231	P; S
11	Ebuloside	C ₂₁ H ₃₁ O ₁₀ [–]	6.50	175	443.19263	443.19117	3.27	Ir		P; S
12	Nonioside k	C ₁₇ H ₂₉ O ₁₁ [–]	7.85		409.17144	409.17191	3.58	Sd		P
13	Glucosyringic acid	C ₁₅ H ₁₉ O ₁₀ [–]	8.56	325	359.09841	359.09824	–0.47	Pa	197.0455 (syringic acid)	P
14	Acetylshikonin	C ₁₈ H ₁₇ O ₆ [–]	9.01	305	329.10162	329.10114	–0.47	Pa	171.07063	P; S
15	Allyl-sucrose	C ₁₅ H ₂₅ O ₁₁ [–]	9.12		381.14023	381.14066	2.86	Sd		P; S
16	Feruloyl-O-galactarate	C ₁₆ H ₁₇ O ₁₁ [–]	9.25	246–310	385.07797	385.07654	3.64	Pa	194.0577, 133.8732	P
17	Cinnamoyl catalpol	C ₂₄ H ₂₇ O ₁₁ [–]	9.29	198	491.15589	491.15479	–1.74	Ir	175.06085	P
18	Cinnamoyl catalpol isomer	C ₁₆ H ₂₁ O ₉ [–]	9.49	198	357.11801	357.11938	–1.74	Ir	258.09830	P; S
19	Linamarin	C ₁₀ H ₁₅ NO ₆ [–]	9.65		246.09821	246.09825	4.21	Sd	258.09830	P
20	Amurensin	C ₂₆ H ₂₉ O ₁₂ [–]	10.03	202–284	533.16431	533.16425	–1.96	Fl	503.14331, 341.1015	P; S
21	2-caffeoylisocitric acid	C ₁₅ H ₁₃ O ₁₀ [–]	9.98		353.07032	353.05173	3.97	Pa	179.06425, 154.99808	P; S
22	Methyl 2,3,4-tris-O-[2-(carboxymethyl) ethyl]-glucose derivative	C ₂₆ H ₃₁ O ₁₃ [–]	10.12		479.17592	479.17749	3.27	Sd		P
23	Methyl 2,3,4-tris-O-[2-(carboxymethyl) ethyl]-glucose	C ₁₉ H ₃₁ O ₁₂ [–]	10.43		451.18228	451.18100	2.83	Sd		P

Table 1. Cont.

Peak	Tentative Identification	[M – H] [–] Ions	Retention Time (min)	UV Max (nm)	Theoretical Mass (m/z)	Measured Mass (m/z)	Accuracy (ppm)	Metabolite Type	MS ² Ions (ppm)	Fruit Part
24	Dimethyl-hydroxyl-oct-2,7-dienoate-glucopyranosyl-glucose	C ₂₂ H ₃₅ O ₁₄ [–]	10.55		523.20213	523.20331	2.24	Sd	241.07164, 125.02764	P; S
25	Aesculetin-7-O-glucuronide	C ₁₅ H ₁₃ O ₁₀ [–]	10.62	232–279–329	353.05140	353.05130	-0.28	Co	177.0193 (Aesculetin)	P; S
26	Hexamethyl-glucopiruronosyl-glucoside methyl ester	C ₁₉ H ₃₃ O ₁₂ [–]	10.83		453.19800	453.19794	2.96	Sd		P
27	7-Hydroxycoumarin glucuronide	C ₁₅ H ₁₃ O ₉ [–]	10.95	255–355	337.05541	337.05661	3.56	Co		P
28	Quercetin-3-O-glucoside-acetate	C ₂₃ H ₂₁ O ₁₃ [–]	11.03	255–355	505.09767	505.09912	2.87	Fl	301.02755 (Quercetin)	P; S
29	Tectoridin	C ₂₂ H ₂₁ O ₁₁ [–]	11.23	281	461.10894	461.10941	3.39	Fl; Is	300.2632 (tectorigenin)	P; S
30	Escopoletin 7-O-glucuronide	C ₁₆ H ₁₅ O ₁₀ [–]	11.35	320	367.06597	367.06729	3.59	Co	171.06593	P; S
31	Hexenyl-xylopiranosyl-glucose	C ₁₇ H ₂₉ O ₁₀ [–]	11.71		393.17706	393.17552	3.91	Sd		P; S
32	Lupinisoflavone A	C ₁₆ H ₁₅ O ₉ [–]	12.12	285	351.07245	351.07106	3.96	Fl; Is	321.0763, 241.0502	P; S
33	2,2,3-Tris (2,3-dihydroxypropanoyl) decanoic acid	C ₁₉ H ₃₁ O ₁₁ [–]	12.43		435.18609	435.18750	3.23	Fa	287.15002	P; S
34	Trimeric proanthocyanidin C2	C ₄₅ H ₃₇ O ₁₈ [–]	12.96	283	865.19859	865.19451	-4.71	Ca	577.1342, (dimer), 289.0714 catechin, (C ₁₅ H ₁₄ O ₆ [–])	P; S
35	Genistein-7-O-di-glucoside	C ₂₇ H ₂₉ O ₁₅ [–]	13.20	230–238–333	593.15122	593.15033	-1.65	Fl; Is	269.0452 (genistein)	P; S
36	Genistein-7-O-di-galactoside	C ₂₇ H ₂₉ O ₁₅ [–]	13.52	230–238–333	593.15120	593.15033	-1.63	Fl; Is	269.0451 (genistein)	P; S
37	Procyanidin B1	C ₃₀ H ₂₃ O ₁₂ [–]	13.83	285	577.13445	577.13373	1.16	Ca	289.0714 catechin, (C ₁₅ H ₁₄ O ₆ [–])	P
38	Genistein-7-O-glucoside	C ₂₁ H ₁₉ O ₁₀ [–]	14.03	230–238–333	431.09847	431.09824	-0.53	Fl; Is	269.0452 (genistein)	P; S
39	Secolonitocide	C ₂₁ H ₃₅ O ₁₂ [–]	14.35		479.21230	479.21350	2.50	Sd		P
40	Trehalose undecylenoate	C ₂₃ H ₃₉ O ₁₂ [–]	15.13		507.24360	507.24454	1.84	Sd	457.06708	P; S
41	Proanthocyanin tetramer	C ₆₀ H ₄₉ O ₂₄ [–]	15.32	285	1153.26191	1153.25146	-9.05	Ca	577.1337 (dimer)	S

Table 1. Cont.

Peak	Tentative Identification	[M – H] [–] Ions	Retention Time (min)	UV Max (nm)	Theoretical Mass (m/z)	Measured Mass (m/z)	Accuracy (ppm)	Metabolite Type	MS ² Ions (ppm)	Fruit Part
42	Bis-2-hydroxyethyl phtalate	C ₁₂ H ₁₃ O ₆ [–]	15.52	315	253.07173	253.07066	4.21	Pa		P; S
43	Daidzein-7-O-galactoside	C ₂₁ H ₁₉ O ₉ [–]	15.63	281	415.10236	415.10327	3.00	Fl; Is	253.05065	P
44	Procyanidin A1	C ₃₀ H ₂₃ O ₁₂ [–]	16.45	282	575.11958	575.11877	–1.42	Ca	289.07157 (catechin)	P; Se
45	Daidzein-7-O-glucoside	C ₂₁ H ₁₉ O ₉ [–]	16.75	230–285–326	415.10236	415.10361	3.00	Fl; Is	273.04050	P; S
46	Ononin (formononetin 7-O-glucoside)	C ₂₂ H ₂₁ O ₉ [–]	17.26	220–285–326	429.11917	429.11880	–0.86	Fl; Is	267.06601, 251.0362 (formononetin)	P
47	1-O-trans-p-coumaroylglycerol	C ₁₂ H ₁₃ O ₆ [–]	17.84	212–326	253.07184	253.07150	–1.34	Pa	119.04922, 120.05251	S
48	1, 3-O-di-trans-p-coumaroylglycerol	C ₂₁ H ₁₉ O ₉ [–]	18.03	212–326	415.10355	415.10333	2.86	Pa	119.04920, 120.05248	P; S
49	Catechin*	C ₁₅ H ₁₃ O ₆ [–]	18.32	285	289.07162	289.07164	0.06	Fl; Ca	260.06575, 245.08210	P; S
50	Tetrahydroxy-tetradecadienoic acid	C ₁₄ H ₂₃ O ₆ [–]	18.45	265	287.15012	287.15001	4.50	Fa		P; S
51	Monic acid A	C ₁₇ H ₂₇ O ₇ [–]	19.03	215	343.17513	343.17657	4.21	Te		P; S
52	Pentahydroxy-octadecatetraoic acid	C ₁₈ H ₂₇ O ₇ [–]	19.47	189	355.17514	355.17648	3.81	Fa		Pu; Se
53	Dictamnolide N	C ₁₈ H ₂₉ O ₈ [–]	19.75	175	373.18569	373.18707	3.69	Te	217.88326	P; S
54	Evodinnol	C ₁₄ H ₁₆ O ₄ [–]	19.83	325	247.09649	247.09760	4.49	Pa	133.02882	P
55	Dihydroxy-pentadecanoic acid	C ₁₅ H ₂₉ O ₄ [–]	20.36	215	273.20724	273.20734	0.36	Fa		P; S
56	12-hydroxyoctadecanoic acid	C ₁₈ H ₃₆ O ₃ [–]	20.52	225	299.25946	299.25807	4.64	Fa		P; S
57	Congestiflorone	C ₂₈ H ₃₁ O ₄ [–]	20.98	243	431.22169	431.22061	–2.49	Be	365.17944, 269.17584, 152.99516	P; S
58	Hydroxy-pentadecaenoic acid	C ₁₅ H ₂₇ O ₄ [–]	21.06	234	271.19144	271.19173	1.06	Fa		P; S
59	Oct-1-en-3-yl-arabinosyl- glucopyranoside	C ₁₉ H ₃₃ O ₁₀ [–]	21.57		421.20821	421.20816	–0.11	Sa		P; S
60	Marrubiin	C ₂₀ H ₂₇ O ₄ [–]	21.73	225	331.19196	331.19039	4.73	Te	207.19521	P

Table 1. Cont.

Peak	Tentative Identification	[M – H] [–] Ions	Retention Time (min)	UV Max (nm)	Theoretical Mass (m/z)	Measured Mass (m/z)	Accuracy (ppm)	Metabolite Type	MS ² Ions (ppm)	Fruit Part
61	Quillaic acid	C ₃₀ H ₄₅ O ₅ [–]	21.85	214	485.32788	485.32615	3.56	Te	405.32125, 249.03424	P; S
62	Dihydroxy-octadecaenoic acid	C ₁₈ H ₃₃ O ₄ [–]	22.05	225	313.23883	313.23734	–4.76	Fa		P; S
63	Pentadecanedioic acid	C ₁₅ H ₂₇ O ₄ [–]	23.25	235	271.19307	271.19165	4.66	Fa		S
64	Trihydroxy-octadecadienoic acid	C ₁₈ H ₃₁ O ₅ [–]	24.21	235	327.21770	327.21780	0.30	Fa		P
65	Trihydroxy-octadecaenoic acid	C ₁₈ H ₃₃ O ₅ [–]	24.68	222	329.23332	329.23341	0.27	Fa		P; S
66	2,3-dihydroxypropyl dodecanoate	C ₁₅ H ₂₉ O ₄ [–]	25.36	198	273.20715	273.20724	4.42	Fa		P; S
67	Tetrahydroxy-heptadecatrienoic acid	C ₁₇ H ₂₇ O ₆ [–]	26.03	285	327.1813	327.18142	3.89	Fa		P; S
68	Jatamanvaltrate H	C ₂₂ H ₃₃ O ₉ [–]	26.19	215	441.21335	441.21329	3.26	Ir	389.62607, 311.22302, 135.04443	P
69	Hydroxy-pentadecanoic acid	C ₁₅ H ₂₉ O ₃ [–]	27.45	235	257.21221	257.21222	0.03	Fa		P; S
70	Unknown	C ₁₄ H ₂₉ O ₈ [–]	28.33	220	325.18569	325.18442	–3.92	Fa		P

Metabolite type: Be: Benzophenones; Ca: Catechins; Co: Coumarins; Fa: Fatty acids; Fl: Flavonoids; Ir: Iridoids; Is: Isoflavones; Oa: Organic acids; Pa: Phenolic acids; Sd: Sugar derivatives; and Tr: Terpenes. Fruit part: P: Pulp and S: Seed.

2.1.1. Coumarins

Several metabolites were identified as coumarins, due to their characteristic UV_{max} spectra. Peak **25** with an anion $[M - H]^-$ (molecule without an hydrogen, charged negatively, formed by the heated electrospray device) at m/z (mass/charge ratio) 353.05130 was identified as aesculetin-7-*O*-glucuronide ($C_{15}H_{13}O_{10}^-$) and peak **27** with a $[M - H]^-$ ion at m/z 337.05643 was identified as 7-hydroxycoumarin-glucuronide ($C_{15}H_{13}O_9^-$). Peak **30**, with a $[M - H]^-$ ion at m/z 367.06696 scopoletin 7-*O*-glucuronide ($C_{16}H_{17}O_{10}^-$).

2.1.2. Flavonoids

Peak **29** with a UV_{max} at 281 nm and with a parent ion at m/z 461.10894 was determined as tectoridin ($C_{22}H_{21}O_{11}^-$). Peak **32** with a similar UV_{max} and a MS ion at m/z 351.08591 was named as lupinisoﬂavone ($C_{20}H_{15}O_6^-$). Peak **35** with an anion $[M - H]^-$ at m/z 593.15024 was determined as genistein-7-*O*-di-glucoside ($C_{27}H_{29}O_{15}^-$) producing a genistein aglycone ion at m/z 269.0452 and peak **36** as a di-galactoside derivative. Peak **38** with a pseudo-molecular ion at m/z 431.09824 was named as genistein-7-*O*-glucoside ($C_{21}H_{19}O_{10}^-$) which produced a MS^2 daughter ion at m/z 269.0452 (genistein). Peaks **43** and **45** with ions around m/z 415.10364 were identified as the isomers: Daidzein-7-*O*-galactoside and glucoside ($C_{21}H_{19}O_9^-$, respectively). Finally, peak **46** was named as ononin (formononetin 7-*O*-glucoside ($C_{22}H_{21}O_9^-$). Peak **20** with an anion $[M - H]^-$ at m/z 533.16435 was determined as amurensin ($C_{26}H_{29}O_{12}^-$), the tert-amyl alcoholic derivative of the flavonol kaempferol 7-*O*-glucoside, while peak **28** with a pseudo-molecular anion at m/z 505.09767 was determined as the related flavonol quercetin-3-*O*-glucoside-acetate ($C_{23}H_{21}O_{13}^-$).

2.1.3. Hydrocarbons and Saturated Organic Acids

Peak **2** was identified as quinic acid ($C_7H_{11}O_6^-$), Peaks **3** and **5** with ions around m/z 191.01933 were determined as citric acid and isocitric acid ($C_6H_7O_7^-$), respectively. Peak **4** with an ion $[M - H]^-$ at m/z 173.00879 was named as dehydroascorbic acid ($C_6H_5O_6^-$), while peak **7** with a $[M - H]^-$ ion at m/z 205.03492 was labeled as homocitric acid ($C_{10}H_{17}O_4^-$). Peak **10** was identified as pantothenic acid.

2.1.4. Oxylipins or Fatty Acids

Several metabolites were identified as polyhydroxylated unsaturated fatty acids known as the dietary antioxidants oxylipins. Accordingly, peak **33** was identified as 2,2,3-Tris(2,3-dihydroxypropanoyl) decanoic acid ($C_{19}H_{31}O_{11}^-$), peak **50** with an anion $[M - H]^-$ at m/z 287.15001 was determined as a tetrahydroxy-tetradecadienoic acid ($C_{14}H_{23}O_6^-$), peak **52** with a $[M - H]^-$ ion at m/z 355.17648 was determined as pentahydroxy-octadecatetraenoic acid ($C_{18}H_{27}O_7^-$), peak **55** with a $[M - H]^-$ ion at m/z 273.20734 was named as dihydroxy-pentadecanoic acid ($C_{15}H_{29}O_4^-$), peak **56** as 12-hydroxyoctadecanoic acid ($C_{18}H_{36}O_3^-$) and peak **58** as its monounsaturated derivative hydroxy-pentadecaenoic acid ion at m/z 271.19173 ($C_{15}H_{27}O_4^-$). Furthermore, peak **62** with an anion $[M - H]^-$ at m/z 313.23734 was reported as dihydroxy-octadecaenoic acid ($C_{18}H_{33}O_4^-$), peak **63** as pentadecanedioic acid ($C_{15}H_{27}O_4^-$) while peak **64** (ion at m/z 327.21780) was identified as trihydroxy-octadecadienoic acid ($C_{18}H_{31}O_5^-$), and peak **65** as trihydroxy-octadecaenoic acid while the related compound peak **67** with an ion at m/z 327.18142 was ascribed to tetrahydroxy-heptadecatrienoic acid ($C_{17}H_{27}O_6^-$). Peak **66** with an anion $[M - H]^-$ at m/z 273.20724 was identified as 2,3-dihydroxypropyl dodecanoate ($C_{15}H_{29}O_4^-$). Peak **65** with an anion $[M - H]^-$ at m/z 329.23341 was assigned to trihydroxy-octadecaenoic acid ($C_{18}H_{33}O_5^-$) as already reported by some of us from the fruits of the *Gomortega keule* (Molina) Baill. (Keule tree). Finally, peak **69** with an anion $[M - H]^-$ at m/z 257.21222 was assigned to hydroxy-pentadecanoic acid ($C_{15}H_{29}O_3^-$) and peak **70** unknown compound matches formula ($C_{14}H_{29}O_8^-$).

2.1.5. Iridoids

Three compounds were identified as iridoids, these compounds are very important because they have exhibited a wide range of bioactive effects, such as hypolipidemic, antioxidant, antimicrobial, hypoglycaemic, choleric, antispasmodic, besides immuno-modulatory anti-inflammatory, neuroprotective, hepatoprotective, and cardioprotective effects [18]. Peak 11 with an ion $[M - H]^-$ at m/z 443.19117 was determined as the iridoid ebuloside ($C_{21}H_{31}O_{10}^-$). Peak 68 with an anion $[M - H]^-$ at m/z 441.21329 was identified as the acylated iridoid jatamanvaltrate H ($C_{22}H_{33}O_9^-$). Peak 17 with an anion $[M - H]^-$ at m/z 491.15479 was determined as cinnamoyl catalpol and peak 18 as its isomer ($C_{24}H_{27}O_{11}^-$).

2.1.6. Terpenes

Several compounds were ascribed as having the terpenoid (C-20 or C-30) skeleton. Peak 9 with an anion $[M - H]^-$ at m/z 365.14422 was tentatively determined as euonyminol ($C_{15}H_{25}O_{10}^-$). Peak 51 with a pseudo-molecular ion at m/z 343.17513 was identified as the terpenoid monic acid ($C_{17}H_{27}O_7^-$) and peak 53 as the sesquiterpene dictamnoid N [19]. Peaks 60 and 61 with ions at m/z 331.19039 and 485.32615 were identified as the diterpene marrubiin ($C_{20}H_{27}O_4^-$) and triterpene quillaic acid ($C_{30}H_{45}O_5^-$), respectively.

2.1.7. Benzophenones

Peak 57 with a pseudo-molecular anion at m/z 431.22061 was identified as the dibenzophenone derivative congestiflorone ($C_{28}H_{31}O_4^-$).

2.1.8. Phenolic Acids and Derivatives

Some eleven compounds were characterized as phenolic acids and derivatives. Peak 1 with an anion $[M - H]^-$ at m/z 377.08671 was determined as syringaldehyde syringate ($C_{18}H_{17}O_9^-$), peak 6 as diffutidin ($C_{17}H_{18}O_5^-$), Peak 8 with a $[M - H]^-$ ion at m/z 329.08671 was labeled as vanilloyl-glucoside ($C_{14}H_{17}O_9^-$), while peak 13 with a $[M - H]^-$ ion at m/z 359.09824 was assigned as glucosyringic acid ($C_{15}H_{19}O_{10}^-$). Peak 14 as acetylshikonic acid ($C_{18}H_{17}O_6^-$), peak 16 with a parent ion at m/z 385.07654 was assigned as *O*-feruloyl-galactarate ($C_{16}H_{17}O_{11}^-$). Peak 21 as 2-caffeoylisocitric acid ($C_{15}H_{13}O_{10}^-$), peak 42 with a $[M - H]^-$ ion at m/z 253.07066 was determined as bis-2-hydroxyethyl phthalate ($C_{12}H_{13}O_6^-$). Some two compounds were identified as phenolic acid glycerol derivatives. Peak 47 with an anion $[M - H]^-$ at m/z 253.07150 was resolved as 1-*O*-*trans*-*p*-coumaroylglycerol ($C_{12}H_{13}O_6^-$) while peak 48 with an anion $[M - H]^-$ at m/z 415.10236 was named as 1,3-*O*-di-*trans*-*p*-coumaroylglycerol ($C_{21}H_{19}O_9^-$) and peak 54 as evodinnol ($C_{14}H_{16}O_4^-$).

2.1.9. Catechins and Proanthocyanidins

Peak 49 with a parent ion at m/z 289.07164 was determined as the flavanol catechin ($C_{15}H_{13}O_6^-$), peak 34 with a parent ion at m/z 865.19451 was resolved as a trimeric procyanidin ($C_{45}H_{37}O_{18}^-$), the fragmentation pattern is in concordance for the trimeric procyanidin C2, ($C_{45}H_{37}O_{18}^-$) isolated from *Pinus radiata* D. Don. Peak 37 with an ion $[M - H]^-$ at m/z 577.13512 was identified as procyanidin B1 ($C_{30}H_{23}O_{12}^-$), while peak 41 with a parent ion $[M - H]^-$ at m/z 1153.25147 was identified as proanthocyanin tetramer ($C_{60}H_{49}O_{24}^-$) and finally, peak 44 was resolved as procyanidin A1 ($C_{30}H_{23}O_{12}^-$).

2.1.10. Sugar Derivatives

The most abundant compounds in *G. sphaelata* fruits were the sugar derivatives. Peak 12 with an ion $[M - H]^-$ at m/z 409.17191 was resolved as the sugar derivative nonioside K ($C_{17}H_{29}O_{11}^-$), while peak 15 with a parent ion $[M - H]^-$ at m/z 381.13914 was determined as allyl-sucrose ($C_{15}H_{25}O_{11}^-$). Peak 22 with a $[M - H]^-$ ion at m/z 479.17749 was

resolved as methyl 2,3,4-tris-*O*-[2-(carboxymethyl) ethyl]-glucose derivative ($C_{26}H_{31}O_{13}^-$) and peak 23 as methyl 2,3,4-tris-*O*-[2-(carboxymethyl) ethyl]-glucose ($C_{19}H_{31}O_{12}^-$). Peak 24 as (*E*)-2,6-dimethyl-6-hydroxyl-oct-2,7-die-noate-2-*O*- β -*D*-glucopyranosyl- β -*D*-glucopyranoside ($C_{22}H_{35}O_{14}^-$). In addition, peak 26 with a parent ion $[M - H]^-$ at m/z 453.19665 was resolved as hexamethyl-glucopyranuronosyl-glucoside methyl ester ($C_{19}H_{33}O_{12}^-$) and peak 31 with a $[M - H]^-$ ion at m/z 393.17552 was determined as hexenyl-xylopyranosyl-glucose ($C_{17}H_{29}O_{10}^-$), peak 39 as secolonitose ($C_{21}H_{35}O_{12}^-$). Finally, peak 59 with a parent ion $[M - H]^-$ at m/z 421.20816 was resolved as oct-1-en-3-yl-arabinosyl-glucopyranoside ($C_{19}H_{33}O_{10}^-$) and peak 40 as Trehalose undecylenoate ($C_{23}H_{39}O_{12}^-$). Peak 19 was identified as linamarin.

2.2. Total Phenolics, Flavonoid Contents, and Antioxidant Activity of *G. sphacelata*

The *in vitro* results of total phenolics, total flavonoid content, and antioxidant activity are summarized in Table 2. DPPH, ABTS, FRAP, and superoxide anion scavenging activity (O_2^-) were used to measure the antioxidant potential in pulp and seed of *G. sphacelata* fruits. These *in vitro* assays are very simple and widely employed to calculate the antioxidant activities of plant and fruit extracts. The results were compared with previous studies from our research as well as work on other Chilean fruits by other researchers [20,21]. The total phenolic contents of pulp of Chilean berries from *G. sphacelata* (45.44 ± 0.67 mg GAE/g dry weight, Table 2) was closer to previous studies reported for the blueberries high-bush type *Vaccinium corimbosum* L (45.86 ± 3.46 mg GAE/g) [20] and Chilean blackberries maqui (*Aristotelia chilensis* (Molina) Stuntz) (49.74 ± 0.57 mg GAE/g) [22]. In addition, our TPC values were almost twice the values for TPC (29 mg Q/g) of the Chilean blackberries *Luma apiculata* (DC.) Burret (commonly known as arrayán or palo colorado) [13]. The amount of TFC found, 35.57 ± 0.86 mg QE/g, was lower than those of Chilean berries *Berberis microphylla* G. Forst. (45.72 ± 2.68 mg QE/g) commonly known as calafate or michay [20]. In the DPPH assay, the trapping capacity of *G. sphacelata* (487.11 ± 26.22 μ mol Trolox/g dry weight) was close to that obtained for the red Chilean berries *Ugni molinae* Turcz. (commonly known as murtila, murta, murtillo, or uñi), (450 μ mol Trolox equivalents, TE/g dry weight) which is considered as an average antioxidant level in the category of edible fruits [21]. The ABTS values (190.32 ± 6.23 μ mol TE/g dry weight) were lower than those of numerous Latin American fruits, such as Chilean blackberries maqui with a trapping capacity of 254.8 ± 8.2 μ mol TE/g dry weight, and Brazilian Acai (*Euterpe oleraceae* Mart.), with 211.0 ± 14 μ mol TE/g dry weight [23], while the FRAP values (169.08 ± 9.81 μ mol TE/g dry weight) were close to those of Acai (157.9 ± 8.7 μ mol TE/g dry weight) [23], but lower than maqui (254.2 ± 2.6 mg TE/g dry weight) [22,23]. The superoxide anion scavenging activity (O_2^-) of *G. sphacelata* ($76.46 \pm 3.18\%$) was higher compared to those established for the blueberries growing in Chile *Vaccinium corimbosum* L. ($72.61 \pm 1.91\%$) [20]. These values can classify these *G. sphacelata* fruits as moderate to high antioxidant small fruits such as plum, cherries, and strawberries [23].

Table 2. Total phenolic contents, total flavonoid contents, and antioxidant activities of *G. sphacelata*.

Sample	TPC ^a	TFC ^b	DPPH ^c	ABTS ^d	FRAP ^e	O_2^- ^f (%)
Pulp	45.44 ± 0.67	35.57 ± 0.86	487.11 ± 26.22	190.32 ± 6.23	169.08 ± 9.81	76.46 ± 3.18 ^b
Seeds	37.21 ± 0.45	28.32 ± 0.35	354.51 ± 34.16	140.49 ± 3.58	147.84 ± 4.35	67.02 ± 2.23 ^b

^a Total phenolic content (TPC), expressed in mg of gallic acid equivalents per gram of dry plant. ^b Total flavonoid content (TFC), expressed in mg of quercetin equivalents per gram of dry plant. ^c 1,1-diphenyl-2-picrylhydrazyl radical (DPPH), as μ mol of Trolox equivalent/g dry fruit, ^d ABTS as μ mol of Trolox equivalent/g dry fruit. ^e Ferric reducing antioxidant power (FRAP), as μ mol TE/g dry weight. ^f Superoxide anion scavenging activity (O_2^-) expressed in %. All values were expressed as means \pm SD ($n = 3$). The results are statistically compared with a positive control. The results were analyzed using one-way analysis of variance (ANOVA) and Tukey test statistical analysis (p -values < 0.05 were regarded as significant). Values in the same column marked with the same letter are not significantly different (at $p < 0.05$).

2.3. In Vitro Cholinesterase Inhibitory Assay

The inhibition of key enzymes, such as AChE and BChE (linked to Alzheimer's disease), is an important metric for identifying novel and safe medicinal value from natural products, especially those found in edible fruits. Indeed, four of the approved anti-Alzheimer drugs are cholinesterase inhibitors. For this reason, we tested the cholinesterase inhibitory potential of *G. sphaelata* against AChE and BChE. The results are shown in Table 3 and expressed as IC₅₀ values. Galantamine was used as a positive control (0.27 ± 0.03 µg/mL against AChE and 3.82 ± 0.02 µg/mL against BChE). *G. sphaelata* fruits showed promising results for both enzymes. In the AChE assay, the inhibition IC₅₀ for pulp was 4.49 ± 0.08 µg/mL and for seeds was 4.38 ± 0.04 µg/mL. As for the BChE assay, the inhibition IC₅₀ for pulp was 73.86 ± 0.09 µg/mL and for seeds was 78.57 ± 0.06 µg/mL. No significant difference was observed.

Table 3. Cholinesterase inhibitory activity of pulp and seed of *G. sphaelata*.

Sample	AChE (IC ₅₀)	BChE (IC ₅₀)
Pulp	4.49 ± 0.08	73.86 ± 0.09
Seeds	4.38 ± 0.04	78.57 ± 0.06
Galantamine	0.27 ± 0.03	3.82 ± 0.02

The results are compared with their positive control. Values correspond to the average of three experiments; all values were expressed as means ± SD. Units of concentrations are expressed as (µg/mL). The results were analyzed using one-way analysis of variance (ANOVA) and Tuckey test statistical analysis (*p*-values < 0.05 were regarded as significant).

Some metabolites contained in *G. sphaelata* have been linked to counteraction against Alzheimer's disease in previous reports. The iridoid jatamanvaltrate H isolated from *V. jatamansi* showed moderate neuroprotective activity [24,25]. In the same way, the crude extract of *V. jatamansi* and its fractions have shown considerable activity against AChE [26]. Marrubiin exhibited potent antinociceptive effects in a dose-dependent manner [27]. Congestiflorone acetates, such as detected in this study, have shown significant inhibitory effects against AChE with an IC₅₀ value at 20.25 ± 0.55 µM [28]. On the other hand, the phenolic glucosyringic acid, did not show significant inhibitory effect on BChE (IC₅₀ > 100 µM) [29]. Catechin presents neuroprotective effects as evidenced by amyloid β-induced neurotoxicity by MTT, lactate dehydrogenase (LDH) release, and neutral red uptake assays [30], but insignificant inhibitory against AChE [31]. Recently, the inhibitory activity against BChE of a procyanidin B1 was reported [32]. To the best of our knowledge, this is the first scientific report regarding the cholinesterase inhibitory potential of *G. sphaelata* fruits.

2.4. Docking Studies

In order to get insights on the intermolecular interactions, the most abundant compounds according to the UHPLC chromatogram (Figure 2) obtained from the pulp and seeds of *G. sphaelata* as well as the known cholinesterase inhibitor galantamine, were subjected to docking assays into the TcAChE catalytic site and hBChE catalytic site. In order to rationalize their pharmacological results analyzing their protein molecular interactions in the light of their experimental inhibition, activities are shown in Table 3. The best docking binding energies expressed in kcal/mol of each compound are shown in Table 4.

Table 4. Binding energies obtained from docking experiments of most abundant compounds in *G. sphacelata*'s fruit and the known cholinesterase inhibitor galantamine over acetylcholinesterase (*TcAChE*) and butyrylcholinesterase (*hBChE*).

Compound	Binding Energy (kcal/mol) Acetylcholinesterase (<i>TcAChE</i>)	Binding Energy (kcal/mol) Butyrylcholinesterase (<i>hBChE</i>)
Quercetin-3- <i>O</i> -glucoside-acetate	−9.46	−8.31
Lupinisoﬂavone	−9.36	−7.99
Genistein-7- <i>O</i> -di-glucoside	−9.18	−6.89
Ononin (formononetin 7- <i>O</i> -glucoside)	−7.45	−6.44
Genistein-7- <i>O</i> -glucoside	−7.24	−5.86
Aesculetin-7- <i>O</i> -glucuronide	−6.67	−6.85
Dihydroxy-octadecaenoic acid	−4.71	−5.76
Hydroxy-pentadecanoic acid	−4.81	−4.87
Galantamine	−11.81	−9.5

2.4.1. Acetylcholinesterase (*TcAChE*) Docking Results

Table 3 showed that the flavonoid quercetin-3-*O*-glucoside-acetate, and the isoflavones lupinisoﬂavone and genistein-7-*O*-di-glucoside displayed the best binding energies of −9.46, −9.36, and −9.18 kcal/mol, respectively. These results suggest that the *G. sphacelata* pulp or seed extracts inhibitory activity over acetylcholinesterase are mainly due the compounds mentioned above, especially the flavonoid quercetin-3-*O*-glucoside-acetate.

Pulp and seeds extract presented considerably abilities to exert an inhibitory potency over the *TcAChE* enzyme ($IC_{50} = 4.49 \pm 0.08$ for pulp extract and $IC_{50} = 4.38 \pm 0.04$ for seeds extract) considering the known cholinesterase inhibitor galantamine (see Table 3). In this sense, Figure 3 shows the hydrogen bond interactions in a two-dimensional diagram of each main and most abundant compounds determined from both extracts into the *TcAChE* catalytic site to summarize the information.

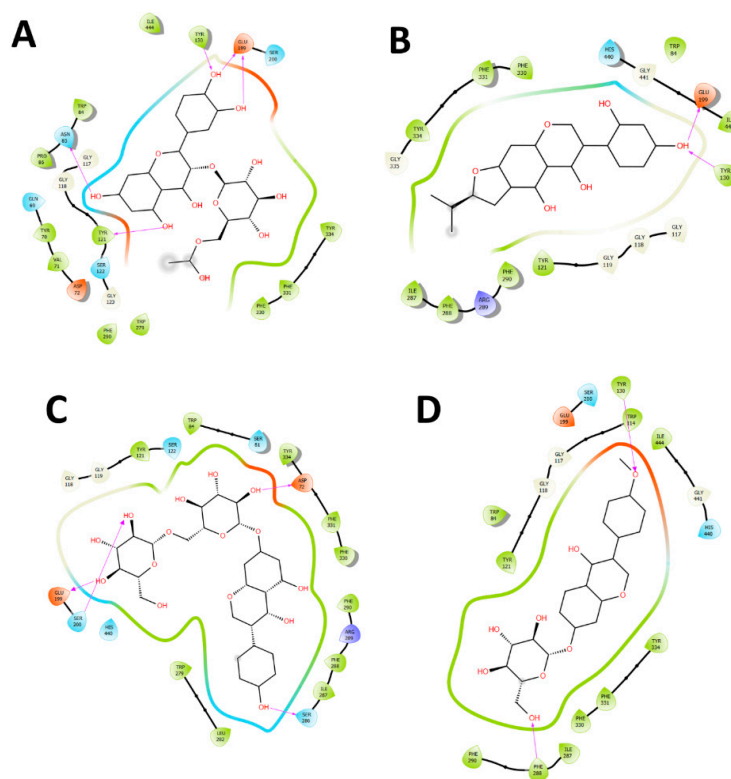


Figure 3. *Cont.*

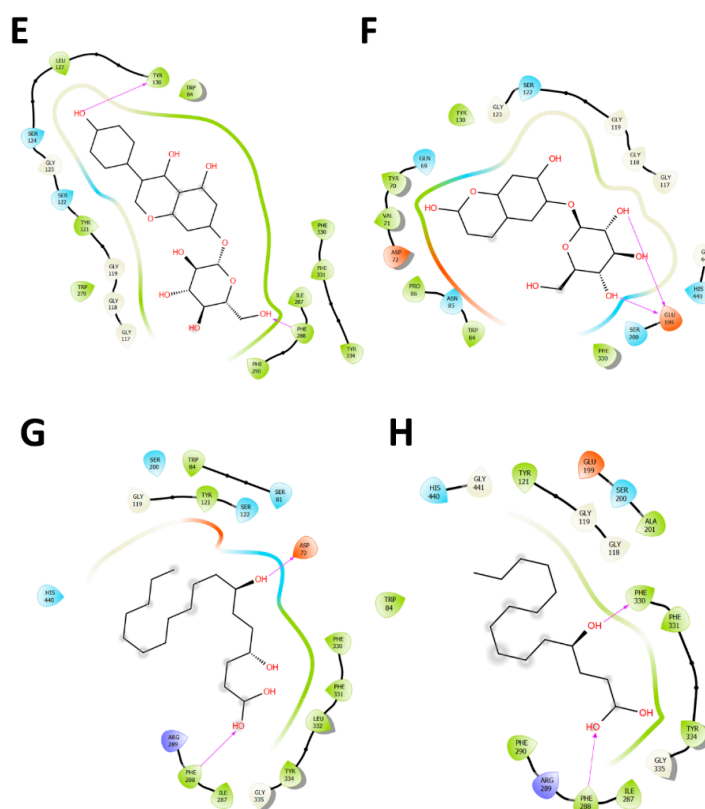


Figure 3. Two-dimensional diagram of *Torpedo californica* acetylcholinesterase (*TcAChE*) catalytic site and hydrogen bond interactions of each main and most abundant compounds obtained from the pulp and seeds extracts. (A) Quercetin-3-*O*-glucoside-acetate (flavonoid); (B) Lupinisoflavone (isoflavone); (C) Genistein-7-*O*-di-glucoside (isoflavone); (D) Ononin (formononetin 7-*O*-glucoside) (isoflavone); (E) Genistein-7-*O*-glucoside (isoflavone); (F) Aesculetin-7-*O*-glucuronide (coumarin); (G) Dihydroxy-octadecaenoic acid (fatty acid); (H) Hydroxy-pentadecaenoic acid (fatty acid).

2.4.2. Butyrylcholinesterase (hBuChE) Docking Results

All binding energies obtained from docking assays over butyrylcholinesterase (*hBChE*) of the most abundant compounds in the pulp and the seeds extracts were shown to be poorer compared to those in *TcAChE*. These results are consistent with the less inhibitory activity of the extracts over this enzyme shown in Table 2 ($IC_{50} = 73.86 \pm 0.09$ for pulp extract and $IC_{50} = 78.57 \pm 0.06$ for seeds extract).

Just like in *TcAChE*, the flavonoid quercetin-3-*O*-glucoside-acetate exhibited the best binding energy profile, suggesting that this derivative could be the main responsible for the inhibitory activity over the *hBChE*.

3. Materials and Methods

3.1. Chemicals and Plant Material

HPLC grade solvents (ethanol, formic acid, and acetonitrile) were obtained from Merck (Santiago, Chile). Ultrapure water was obtained from a water system of purification (Milli-Q Merck Millipore, Chile). Flavonol standards (catechin, isoflavones, and flavonoids, with a high purity: 95% by HPLC) were acquired from ChromaDex (Santa Ana, CA, USA), Sigma-Aldrich (Saint Louis, Mo, USA), or Extrasynthèse (Genay, France). Folin-Ciocalteu reagent, NaOH, Na_2CO_3 , $AlCl_3$, $FeCl_3$, HCl, $NaNO_2$, trichloroacetic acid, quercetin, Trolox sodium acetate, gallic acid, 2,4,6-tri(2-pyridyl)-s-triazine (TPTZ), nitroblue tetrazolium, xanthine oxidase, and DPPH (1,1-diphenyl-2-picrylhydrazyl radical), acetylcholinesterase (AChE) from electric eel (*Torpedo californica*), butylcholinesterase (BChE) from

horse serum, 5,5'-dithiobis(2-nitrobenzoic) acid (DTNB), acetylthiocholine iodide, butyrylthiocholine chloride, and galantamine were purchased from Sigma-Aldrich Chemical Company (Santiago, Chile). *G. sphacelata* fruits were collected in November 2016 in Valdivia, XIV Region de Los Ríos, Chile. The fruits were identified by Jorge Macaya (Universidad de Chile) and a voucher specimen were kept at the Institute of Pharmacy of the Universidad Austral de Chile under number GS20161115.

3.2. Fruit Processing

Five g of pulp and seeds, separately, were chopped and lyophilized (FreeZone 2.5 L Labconco, USA). The material was extracted (20% *w/v*) with a mixture of ethanol-distilled water (1:1 *v/v*) as solvent (at 25 °C, for two h in an ultrasonic bath). The extract was filtered, and the solvent was evaporated under vacuum at 45 °C. The extract was frozen and lyophilized, until a yield of 327.3 and 125.8 mg of dark brown gums (6.54 and 2.51%) from pulp and seeds, respectively.

3.3. UHPLC-PDA-Orbitrap-MS

The Dionex Thermo Scientific Ultimate 3000 UHPLC system connected with a Thermo Q Exactive Focus machine was used as previously informed [33]. Samples were re-dissolved (2 mg/mL) in ethanol-distilled water (1:1 *v/v*) and 10 µL of filtered solution (PTFE filter) were injected in the instrument, as previously discussed [33].

3.4. LC Parameters and MS Parameters

Liquid chromatography (LC) was executed by a C-18 Acclaim UHPLC column (×4.6 mm ID 150 mm, 2.5 µm, Thermo Fisher Scientific, Bremen, Germany) set at 25 °C. The wavelength detection was set at: 280, 354, 254, and 330 nm, and DAD was attained from 200 to 800 nm for full characterization of peaks. Mobile phases employed were acetonitrile (B) and 1% formic aqueous solution (A) while the gradient program was: (0.00 min, 5% B); (5.00 min, 5% B); (10.00 min, 30% B); (15.00 min, 30% B); (20.00 min, 70% B); (25.00 min, 70% B); (35.00 min, 5% B); and 12 min for column equilibration before injections. The flow rate employed was 1.00 mL min⁻¹, and the injection volume was 10 µL. Standards and the fruit extracts dissolved in methanol were maintained at 10 °C during storage in the auto-sampler. The HESI II and Orbitrap spectrometer parameters were set as informed previously [34].

3.5. Total Phenolic (TP) and Total Flavonoid (TF) Content

The total phenolic contents and total flavonoid content of the *G. sphacelata* fruits were measured using the Folin-Ciocalteu and FeCl₃ method previously described by our work with some modifications [35]. For TP, the results were expressed as mg of gallic acid equivalents per gram of dry fruit. While for the TF content results were presented as mg of quercetin equivalents per gram of dry fruit. The determination was performed using a Synergy HTX microplate reader (Biotek, Winoosky, VT, USA), in triplicate and reported as the mean ± SD.

3.6. Antioxidant Assays

3.6.1. DPPH Cation Radical Discoloration Test

The method previously reported by Brand-Williams et al., was used to determine radical DPPH scavenging activity. Briefly, 2 mL of the DPPH solution was added in 400 µL of the extract (2 mg/mL) and mixed and 1.10 ± 0.02 at 517 nm absorbance was adjusted with methanol. This homogenized mixture of fruit extract and DPPH solution was then kept in a dark environment for a period of 20 min at room temperature [36]. Finally, the absorbance was calculated at 517 nm. The inhibition percentage was measured by a given formula:

$$\text{Percentage Inhibition} = [1 - (\text{S.A/B.A})] \times 100 \quad (1)$$

where S.A. is sample absorbance and B.A. is used for blank absorbance.

3.6.2. Bleaching Test with the Cationic Radical ABTS^{•+}

The ABTS^{•+} radical capacity was evaluated using the decolorization method described by Kuskoski et al., 2004 [37]. The ABTS solution (7 mM) and potassium persulfate (2.45 mM) solution were prepared and mixed in a ratio of 1:1. The resultant solution was incubated for 16 h. Using 96-well plates, 275 µL of the solution (absorbance 0.7) was mixed with 25 µL of samples/standard. The absorbances were measured at 734 nm after 6 min of incubation period at 30 °C using a Synergy HTX microplate reader. Results were expressed as µmol Trolox per milliliters.

3.6.3. Ferric Reduction Ability-Antioxidant Power Test (FRAP)

The FRAP test was performed with the previously described protocol by Benzie and Strain, with a slight modification [38]. Briefly, the FRAP solution (2 mL) mixed with 200 µL of extract (2 mg/mL), was stirred and kept in the dark for 5 min. The absorbance was measured at 595 nm.

3.6.4. Superoxide Anion Scavenging Assay

The assay was carried using xanthine oxidase and hypoxanthine, and the absorbances were measured at 560 nm according to the reported with some modifications [13]. The production of the enzyme xanthine oxidase of superoxide anion radical (O₂⁻) reduces the NBT (nitro blue tetrazolium) dye, producing a chromophore that absorbs at 520 nm. The superoxide anion trapping capacities of the extracts were measured using a Synergy HTX microplate reader (Biotek, CA, USA).

3.7. Cholinesterases (ChE) Inhibitory Activity

Ellman's method was used to determinate the inhibitory activity of *G. sphacelata* fruits [39]. DTNB was dissolved in Tris HCl (pH 8) containing 0.02 M of MgCl₂ and 0.1 M NaCl. The sample solution (50 mL dH₂O, 2 mg L⁻¹) was mixed with DTNB (125 mL), acetylcholinesterase (AChE; or BChE) (25 mL), while the blank sample as a control contained all the solutions except enzymes and was distributed in a 96-well microplate. The acetyl-thiocholine iodide (ATCI) or butyryl-thiocholine chloride (BTCl) (25 mL) was added to start the reaction. The reading was taken on a 405 nm absorbance after incubation at 25 °C for 15 min. The cholinesterase inhibitory activity was measured as IC₅₀ (µg mL⁻¹, concentration range 0.05 to 25 µg mL⁻¹) by subtracting the absorbance of the sample from blank. Galantamine was used as a positive control. All data were collected in triplicate. In addition, 0.26 units/mL of each enzyme were used for the inhibition assays.

3.8. Docking Studies

The geometries and partial charges of several representative compounds contained in the extracts, as well as the known cholinesterases (*TcAChE*- *hBChE*) inhibitor Galantamine were fully optimized using the DFT method with the standard basis set PBEPBE/6-311 + g* [40,41]. All calculations were performed in the Gaussian 09W software.

3.9. Statistical Analysis

All the experiments were repeated five times to confirm the results and minimize the error and the data was presented as the mean of standard deviation. The results were analyzed using one-way analysis of variance (ANOVA) and Tuckey test statistical analysis (*p*-values < 0.05 were regarded as significant) using the origin Pro 9.0 software package (Origin lab Corporation, Northampton, MA, USA).

4. Conclusions

From the edible endemic Chilean *G. sphacelata* fruit seventy metabolites were detected using UHPLC-PDA-Orbitrap-MS analysis including phenolic acids, organic acids, sugar derivatives, catechins, proanthocyanidins, fatty acids, iridoids, coumarins, a benzophenone, flavonoids, and terpenes. *G. sphacelata* showed a good phenolic content and moderate antioxidant and enzyme inhibitory activities. This report could contribute for the better understanding of chemistry and biological activities in the genus *Greigia*. Furthermore, the list of compounds profiled with a cholinesterase inhibitory activity plus antioxidant potential make *G. sphacelata* fruits an interesting source of compounds with interesting properties to prepare functional foods or food derived supplements.

Supplementary Materials: The following are available online. Figure S1 (a–v): Full MS spectra and structures of compounds 1, 3, 7, 9, 12, 13, 15, 25, 27, 28, 29, 35, 37, 42, 43, 44, 46, 48, 51, 53, and 55; Table S1: Binding energies obtained from docking experiments of most abundant compounds in *G. sphacelata*'s fruit and the known cholinesterase inhibitor galantamine over acetylcholinesterase (*TcAChE*) and butyrylcholinesterase (*hBuChE*); Figure S2: Components of *G. sphacelata* fruits used in docking studies Figure S3: Predicted binding mode and predicted intermolecular interactions of all most abundant compounds in *G. sphacelata* pulp and seeds extracts and the residues of *Torpedo californica* acetylcholinesterase (*TcAChE*) catalytic site; Figure S4: Predicted binding mode and predicted intermolecular interactions of all most abundant compounds in *G. sphacelata* pulp and seeds extracts and the residues of human butyrylcholinesterase (*hBuChE*) catalytic site.

Author Contributions: R.E.B., S.A., and C.C. performed the LC-MS experiments and antioxidant and enzyme inhibitory assays; J.R.-P. performed the docking experiments; M.J.S., C.F.-G., S.A., and J.E. arranged the data and wrote the manuscript. All authors have read and agreed to the published version of the manuscript.

Funding: This research received funds from FONDECYT 1180059 and CONICYT PFCHA/beca doctorado nacional/2019-21191978. J.E. gratefully acknowledges funding from CONICYT (PAI/ACADEMIA No. 79160109). Postdoctorate grants 3190794 (C.F.-G.) and 3190572 (S.A.) are gratefully acknowledged.

Acknowledgments: We acknowledge Milena Rios for her help in vitro microplate assays.

Conflicts of Interest: The authors declare no conflict of interest.

References

1. Slavin, J.L.; Lloyd, B. Health benefits of fruits and vegetables. *Adv. Nutr.* **2012**, *3*, 506–516. [[CrossRef](#)] [[PubMed](#)]
2. Yeung, A.W.K.; Aggarwal, B.B.; Barreca, D.; Battino, M.; Belwal, T.; Horbańczuk, O.K.; Berindan-Neagoe, I.; Bishayee, A.; Daglia, M.; Devkota, H.P.; et al. Dietary natural products and their potential to influence health and disease including animal model studies. *Anim. Sci. Pap. Rep.* **2019**, *36*, 345–358.
3. Afrin, S.; Giampieri, F.; Gasparrini, M.; Forbes-Hernandez, T.Y.; Varela-López, A.; Quiles, J.L.; Mezzetti, B.; Battino, M. Chemopreventive and Therapeutic Effects of Edible Berries: A Focus on Colon Cancer Prevention and Treatment. *Molecules* **2016**, *21*, 169. [[CrossRef](#)] [[PubMed](#)]
4. Forino, M.; Tartaglione, L.; Dell'Aversano, C.; Ciminiello, P. NMR-based identification of the phenolic profile of fruits of *Lycium barbarum* (goji berries). Isolation and structural determination of a novel N-feruloyl tyramine dimer as the most abundant antioxidant polyphenol of goji berries. *Food Chem.* **2016**, *194*, 1254–1259. [[CrossRef](#)]
5. Belwal, T.; Bisht, A.; Devkota, H.P.; Ullah, H.; Khan, H.; Pandey, A.; Bhatt, I.D.; Echeverría, J. Phytopharmacology and clinical updates of *Berberis* species against diabetes and other metabolic diseases. *Front. Pharm.* **2020**, *11*, 41. [[CrossRef](#)]
6. Areche, C.; Hernandez, M.; Cano, T.; Ticona, J.; Cortes, C.; Simirgiotis, M.; Caceres, F.; Borquez, J.; Echeverría, J.; Sepulveda, B. *Corryocactus brevistylus* (K. Schum. ex Vaupel) Britton & Rose (Cactaceae): Antioxidant, gastroprotective effects, and metabolomic profiling by ultrahigh-pressure liquid chromatography and electrospray high resolution orbitrap tandem mass spectrometry. *Front. Pharm.* **2020**, *11*, 417. [[CrossRef](#)]
7. Zhang, Q.; Chen, W.; Zhao, J.; Xi, W. Functional constituents and antioxidant activities of eight Chinese native goji genotypes. *Food Chem.* **2016**, *200*, 230–236. [[CrossRef](#)]
8. Simirgiotis, M.J.; Ramirez, J.E.; Schmeda Hirschmann, G.; Kennelly, E.J. Bioactive coumarins and HPLC-PDA-ESI-ToF-MS metabolic profiling of edible queule fruits (*Gomortega keule*), an endangered endemic Chilean species. *Food Res. Int.* **2013**, *54*, 532–543. [[CrossRef](#)]

9. Li, J.; Yuan, C.; Pan, L.; Benatrehina, P.A.; Chai, H.; Keller, W.J.; Naman, C.B.; Kinghorn, A.D. Bioassay-guided isolation of antioxidant and cytoprotective constituents from a maqui berry (*Aristotelia chilensis*) dietary supplement ingredient as markers for qualitative and quantitative analysis. *J. Agric. Food Chem.* **2017**, *65*, 8634–8642. [[CrossRef](#)]
10. Will, B.; Zizka, G.A. Review of the genus *Greigia* Regel (Bromeliaceae) in Chile. *Harv. Pap. Bot.* **1999**, *4*, 225–239.
11. Flagg, M.L.; Wächter, G.A.; Davis, A.L.; Montenegro, G.; Timmermann, B.N. Two novel flavanones from *Greigia sphacelata*. *J. Nat. Prod.* **2000**, *63*, 1689–1691. [[CrossRef](#)] [[PubMed](#)]
12. Donno, D.; Beccaro, G.L.; Mellano, M.G.; Cerutti, A.K.; Bounous, G. Goji berry fruit (*Lycium* spp.): Antioxidant compound fingerprint and bioactivity evaluation. *J. Funct. Foods* **2015**, *18*, 1070–1085. [[CrossRef](#)]
13. Simirgiotis, M.J.; Bórquez, J.; Schmeda-Hirschmann, G. Antioxidant capacity, polyphenolic content and tandem HPLC-DAD-ESI/MS profiling of phenolic compounds from the South American berries *Luma apiculata* and *L. chequen*. *Food Chem.* **2013**, *139*, 289–299. [[CrossRef](#)] [[PubMed](#)]
14. Fu, C.; Liu, M.; Li, Y.; Wang, K.; Yang, B.; Deng, L.; Tian, J.; Yang, G.; Zheng, G. UPLC-Q-exactive orbitrap MS analysis for identification of lipophilic components in citri sarcodactylis fructus from different origins in China using supercritical CO₂ fluid extraction method. *ACS Omega* **2020**, *5*, 11013–11023. [[CrossRef](#)]
15. Barrientos, R.; Fernández-Galleguillos, C.; Pastene, E.; Simirgiotis, M.; Romero-Parra, J.; Ahmed, S.; Echeverría, J. Metabolomic analysis, fast isolation of phenolic compounds, and evaluation of biological activities of the bark from *Weinmannia trichosperma* Cav. (Cunoniaceae). *Front. Pharm.* **2020**, *11*, 780. [[CrossRef](#)]
16. Spínola, V.; Mendes, B.; Câmara, J.S.; Castilho, P.C. An improved and fast UHPLC-PDA methodology for determination of L-ascorbic and dehydroascorbic acids in fruits and vegetables. Evaluation of degradation rate during storage. *Anal. Bioanal. Chem.* **2012**, *403*, 1049–1058.
17. Lim, V.; Gorji, S.G.; Daygon, V.D.; Fitzgerald, M. Untargeted and targeted metabolomic profiling of australian indigenous fruits. *Metabolites* **2020**, *10*, 114. [[CrossRef](#)]
18. Dinda, B. Pharmacology of Iridoids. In *Pharmacology and Applications of Naturally Occurring Iridoids*; Dinda, B., Ed.; Springer International Publishing: Cham, Switzerland, 2019; pp. 145–254. ISBN 978-3-030-05575-2.
19. Chang, J.; Xuan, L.J.; Xu, Y.M.; Zhang, J.S. Seven new sesquiterpene glycosides from the root bark of *Dictamnus dasycarpus*. *J. Nat. Prod.* **2001**, *64*, 935–938. [[CrossRef](#)]
20. Ramirez, J.E.; Zambrano, R.; Sepúlveda, B.; Kennelly, E.J.; Simirgiotis, M.J. Anthocyanins and antioxidant capacities of six Chilean berries by HPLC–HR-ESI-ToF-MS. *Food Chem.* **2015**, *176*, 106–114. [[CrossRef](#)]
21. Rodríguez, K.; Ah-Hen, K.; Vega-Gálvez, A.; López, J.; Quispe-Fuentes, I.; Lemus-Mondaca, R.; Gálvez-Ranilla, L. Changes in bioactive compounds and antioxidant activity during convective drying of murta (*Ugni molinae* T.) berries. *Int. J. Food Sci. Technol.* **2014**, *49*, 990–1000. [[CrossRef](#)]
22. Genskowsky, E.; Puente, L.A.; Pérez-Álvarez, J.A.; Fernández-López, J.; Muñoz, L.A.; Viuda-Martos, M. Determination of polyphenolic profile, antioxidant activity and antibacterial properties of maqui [*Aristotelia chilensis* (Molina) Stuntz] a Chilean blackberry. *J. Sci. Food Agric.* **2016**, *96*, 4235–4242. [[CrossRef](#)] [[PubMed](#)]
23. Gironés-Vilaplana, A.; Baenas, N.; Villaño, D.; Speisky, H.; García-Viguera, C.; Moreno, D.A. Evaluation of Latin-American fruits rich in phytochemicals with biological effects. *J. Funct. Foods* **2014**, *7*, 599–608. [[CrossRef](#)]
24. Xu, J.; Guo, Y.; Xie, C.; Jin, D.-Q.; Gao, J.; Gui, L. Isolation and neuroprotective activities of acylated iridoids from *Valeriana jatamansi*. *Chem. Biodivers.* **2012**, *9*, 1382–1388. [[CrossRef](#)] [[PubMed](#)]
25. Xu, J.; Li, Y.; Guo, Y.; Guo, P.; Yamakuni, T.; Ohizumi, Y. Isolation, structural elucidation, and neuroprotective effects of iridoids from *Valeriana jatamansi*. *Biosci. Biotechnol. Biochem.* **2012**, *76*, 1401–1403. [[CrossRef](#)]
26. Jugran, A.K.; Rawat, S.; Bhatt, I.D.; Rawal, R.S. *Valeriana jatamansi*: An herbaceous plant with multiple medicinal uses. *Phyther. Res.* **2019**, *33*, 482–503. [[CrossRef](#)]
27. De Jesus, R.A.P.; Cechinel-Filho, V.; Oliveira, A.E.; Schlemper, V. Analysis of the antinociceptive properties of marrubiin isolated from *Marrubium vulgare*. *Phytomedicine* **2000**, *7*, 111–115. [[CrossRef](#)]
28. Teh, S.S.; Ee, G.C.L.; Mah, S.H.; Ahmad, Z. Structure–activity relationship study of secondary metabolites from *Mesua beccariana*, *Mesua ferrea* and *Mesua congestiflora* for anti-cholinesterase activity. *Med. Chem. Res.* **2016**, *25*, 819–823. [[CrossRef](#)]

29. Woo, M.H.; Nguyen, D.H.; Choi, J.S.; Park, S.E.; Thuong, P.T.; Min, B.S.; Le, D.D. Chemical constituents from the roots of *Kadsura coccinea* with their protein tyrosine phosphatase 1B and acetylcholinesterase inhibitory activities. *Arch. Pharm. Res.* **2020**, *43*, 204–213. [[CrossRef](#)]
30. Kim, J.H.; Choi, G.N.; Kwak, J.H.; Jeong, H.R.; Jeong, C.-H.; Heo, H.J. Neuronal cell protection and acetylcholinesterase inhibitory effect of the phenolics in chestnut inner skin. *Food Sci. Biotechnol.* **2011**, *20*, 311–318. [[CrossRef](#)]
31. Gilani, A.H.; Ghayur, M.N.; Saify, Z.S.; Ahmed, S.P.; Choudhary, M.I.; Khalid, A. Presence of cholinomimetic and acetylcholinesterase inhibitory constituents in betel nut. *Life Sci.* **2004**, *75*, 2377–2389. [[CrossRef](#)]
32. Floris, S.; Fais, A.; Rosa, A.; Piras, A.; Marzouki, H.; Medda, R.; González-Paramás, A.M.; Kumar, A.; Santos-Buelga, C.; Era, B. Phytochemical composition and the cholinesterase and xanthine oxidase inhibitory properties of seed extracts from the *Washingtonia filifera* palm fruit. *RSC Adv.* **2019**, *9*, 21278–21287. [[CrossRef](#)]
33. Simirgiotis, J.M.; Quispe, C.; Bórquez, J.; Areche, C.; Sepúlveda, B. Fast detection of phenolic compounds in extracts of easter pears (*Pyrus communis*) from the Atacama Desert by ultrahigh-performance liquid chromatography and mass spectrometry (UHPLC–Q/Orbitrap/MS/MS). *Molecules* **2016**, *21*, 92. [[CrossRef](#)] [[PubMed](#)]
34. Simirgiotis, M.J.; Quispe, C.; Bórquez, J.; Schmeda-Hirschmann, G.; Avendaño, M.; Sepúlveda, B.; Winterhalter, P. Fast high resolution Orbitrap MS fingerprinting of the resin of *Heliotropium taltalense* Phil. from the Atacama Desert. *Ind. Crop. Prod.* **2016**, *85*, 159–166. [[CrossRef](#)]
35. Quesada-Romero, L.; Fernández-Galleguillos, C.; Bergmann, J.; Amorós, M.-E.; Jiménez-Aspee, F.; González, A.; Simirgiotis, M.; Rossini, C. Phenolic fingerprinting, antioxidant, and deterrent potentials of *Persicaria maculosa* Extracts. *Molecules* **2020**, *25*, 3054. [[CrossRef](#)]
36. Brand-Williams, W.; Cuvelier, M.E.; Berset, C. Use of a free radical method to evaluate antioxidant activity. *LWT Food Sci. Technol.* **1995**, *28*, 25–30. [[CrossRef](#)]
37. Kuskoski, E.M.; Asuero, A.G.; García-Parilla, M.C.; Troncoso, A.M.; Fett, R. Actividad antioxidante de pigmentos antocianicos. *Ciênc. E Tecnol. Aliment.* **2004**, *24*, 691–693. [[CrossRef](#)]
38. Benzie, I.; Strain, J.J. The ferric reducing ability of plasma (FRAP) as a measure of “antioxidant power”: The FRAP assay. *Anal. Biochem.* **1996**, *239*, 70–76. [[CrossRef](#)]
39. Mocan, A.; Moldovan, C.; Zengin, G.; Bender, O.; Locatelli, M.; Simirgiotis, M.; Atalay, A.; Vodnar, D.C.; Rohn, S.; Crişan, G. UHPLC-QTOF-MS analysis of bioactive constituents from two Romanian Goji (*Lycium barbarum* L.) berries cultivars and their antioxidant, enzyme inhibitory, and real-time cytotoxicological evaluation. *Food Chem. Toxicol.* **2018**, *115*, 414–424. [[CrossRef](#)]
40. Adamo, C.; Barone, V. Toward reliable density functional methods without adjustable parameters: The PBE0 model Seeking for parameter-free double-hybrid functionals: The PBE0-DH model accurate excitation energies from time-dependent density functional theory: Assessing the PBE0 model toward reliable density functional methods without adjustable parameters: The PBE0 model. *Cit. J. Chem. Phys.* **1999**, *110*, 2889. [[CrossRef](#)]
41. Petersson, G.A.; Bennett, A.; Tensfeldt, T.G.; Al-Laham, M.A.; Shirley, W.A.; Mantzaris, J. A complete basis set model chemistry. I. The total energies of closed-shell atoms and hydrides of the first-row elements. *J. Chem. Phys.* **1988**, *89*, 2193–2218. [[CrossRef](#)]

Sample Availability: The datasets generated during and/or analyzed during the current study are available from the corresponding author on reasonable request.



© 2020 by the authors. Licensee MDPI, Basel, Switzerland. This article is an open access article distributed under the terms and conditions of the Creative Commons Attribution (CC BY) license (<http://creativecommons.org/licenses/by/4.0/>).